Original article

MOLECULAR METABOLISM

Depot specific differences in the adipogenic potential of precursors are mediated by collagenous extracellular matrix and Flotillin 2 dependent signaling

Gerald Grandl [1], Sebastian Müller [1,2], Hansjörg Moest [1,2], Caroline Moser [1], Bernd Wollscheid [2], Christian Wolfrum [1,*]

ABSTRACT

Objective: Adipose tissue shows a high degree of plasticity, and adipocyte hyperplasia is an important mechanism for adipose tissue expansion. Different adipose depots respond differently to an increased demand for lipid storage. Orchestrating cellular expansion in vivo requires extracellular matrix (ECM) remodeling and a high degree of interaction between cells and ECM.

Methods: We studied decellularized primary adipose stromal cell derived ECM of different adipose depots and reseeded them with primary adipose precursors. We tested ECM effect on adipocyte differentiation and analyzed ECM composition using proteomic and immunohistochemical approaches to identify factors in the ECM influencing adipogenesis.

Results: We show that the ECM of an adipose depot is the major determinant for the differentiation capacity of primary preadipocytes. Visceral adipose tissue stromal cells differentiate less than subcutaneous cells, which, in turn, are less adipogenic than BAT-derived cells. This effect is based on the ECM composition of the respective depot and not dependent on the precursor origin. Addition of vitamin C pronounces the pro-adipogenic effects of the ECM, indicating the importance of collagenous ECM in mediating the effect. Using a proteomic global and a targeted downstream analysis, we identify Flotillin 2 as a protein enriched in pro-adipogenic ECM, which is involved in orchestrating ECM to preadipocyte signaling.

Conclusions: We show that adipose tissue SVF secretes collagenous ECM, which directly modulates terminal differentiation of adipocyte precursors in a depot specific manner. These data demonstrate the importance of the tissue microenvironment in preadipocyte differentiation.

Keywords Adipocyte precursors; Extracellular matrix; Collagen; Stem cell niche; Flotillin 2

1. INTRODUCTION

The global prevalence of obesity, which is an excessive expansion of an individual's adipose tissue stores, has been rising at an alarming rate over the last decades and is predicted to reach even higher proportions in the future [1]. Adipose tissue (AT) can be broadly categorized into white AT (WAT) and brown AT (BAT), with white AT further separated into subcutaneous (Sc) and visceral (Vis) AT, which is localized inside the peritoneal cavity. The main cell type of AT is the terminally differentiated adipocyte, which is composed of a small cytosol and one or more large lipid droplets for triglyceride storage. The AT stroma contains tissue resident fibroblasts, endothelial, and smooth muscle cells as well as macrophages [2].

AT shows a high degree of plasticity and is able to respond to an increased demand to store calories with rapid expansion. The two modes of AT expansion are hypertrophy, which is an increase in cell size, and hyperplasia, which is an increase in cell number. Increasing the number of adipocytes requires the activation of tissue resident adipose precursor cells, which are believed to be of a mesenchymal origin and give rise to committed preadipocytes. Tracing studies using a PPARγ-GFP mouse line initially identified adipocyte precursor cells to be of perivascular origin [3]. The first defined population of AT resident fibroblasts thought to be committed preadipocytes was identified in 2008 [4], and has since been specified further [5]. Further studies have revealed a Lin- PDGFRα+ fibroblast residing in AT perivascular space that is able to give rise to both brown and white adipocytes [6].

Terminal differentiation of preadipocytes is a complex process critically involving the nuclear receptor PPARγ [7] and entails the morphological change from a fibroblast-type precursor to a round, large cell filled with lipid droplets for triglyceride storage. In addition to this, the interaction of the differentiating cell with its surrounding extracellular matrix (ECM), as well as extensive ECM remodeling, plays an important role in this process [8,9].

[1]Institute of Food, Nutrition and Health, ETH Zurich, Schwerzenbach, Switzerland [2]Institute of Molecular Systems Biology, ETH Zürich, Switzerland

*Corresponding author. ETH Zürich, Schorenstrasse 16, CH-8603 Schwerzenbach, Switzerland. E-mail: christian-wolfrum@ethz.ch (C. Wolfrum).

Received July 11, 2016 • Revision received July 20, 2016 • Accepted July 25, 2016 • Available online 30 July 2016

http://dx.doi.org/10.1016/j.molmet.2016.07.008

Involvement of ECM in orchestrating the correct response of tissue resident cells to various stimuli has become a focus of intense study, and various ECM properties have been shown to directly influence precursor or stem cell behavior [10]. In addition, prolonged states of inflammation, tissue damage, or remodeling often lead to a state termed fibrosis, which is excessive deposition of ECM, and is frequently observed concomitantly with high levels of obesity and dysfunctional adipose tissue [11].

In obesity, a physiological environment favoring AT expansion, different adipose depots have been shown to expand differently. Sc AT grows slower and shows more of a hyperplastic response while Vis AT grows more rapidly and shows more extensive hypertrophy. To some extent, these two modes of expansion also correlate with clinical outcomes, where hypertrophic Vis AT is associated with poor metabolic health while Sc AT is sometimes ascribed a beneficial role [12].

Given the important role ECM is known to play in terminal differentiation of preadipocytes, as well as the known differences in the response of different adipose depots, we employed a strategy of deriving the extracellular matrix from primary cells of different adipose depots to investigate its role in adipose precursor differentiation.

2. MATERIAL AND METHODS

2.1. Materials

All chemicals were purchased from Sigma–Aldrich unless specified otherwise.

2.2. Animals

C57Bl/6 mice were housed in a pathogen-free animal facility on a 12-h/12-h light/dark cycle with free access to food and water, at an ambient temperature of 23 °C.

2.3. Western blot analysis

Whole cell lysates were prepared as previously described [13]. For western blot analysis, the following antibodies were used: FLOT2 (Santa Cruz Biotechnology, SC-25507, 1:1000) and Hsp90 (Cell Signalling Technology, #4877 S).

2.4. Cell culture

All cells were cultured in high-glucose DMEM supplemented with 10% fetal bovine serum and 1% penicillin/streptomycin (all Invitrogen). 3T3-L1 cells or primary SVF were seeded onto plates coated with cross-linked gelatin and grown to confluence prior to differentiation. Two days post-confluence, cells were treated with induction cocktail (1 μg/ml insulin, 1 μM dexamethasone and 115 μg/ml isobutylmethylxanthine) for 2 days followed by insulin media (1 μg/ml insulin) for 2 days and DMEM for 3 days. For ECM reseeding, FACS-sorted cells were plated into decellularized ECM at 50 000 or 100 000 cells per well. For FLOT2 knockdown the siRNA TGGGCAAGAACGTACAGGACATTAA and a scrambled control were used at 100 nM.

2.5. Primary cell isolation

For SVF preparation, adipose tissue subcutaneous (inguinal), visceral (perigonadal), and brown (interscapular) fat pads were dissected, finely minced, and incubated with collagenase (1 mg/ml) in collagenase buffer (25 mM NaHCO3, 12 mM KH2PO4, 1.2 mM gSO4 1.2 mM, 4.8 mM KCl 120 mM NaCl, 1.4 mM CaCl2 5 mM Glucose, BSA 2.5%, pH = 7.4) for 1 h at 37 °C. Cells were washed in DMEM, 10% FBS and filtered through 40 μM cell strainers; erythrocytes were lysed by washing in erythrocyte lysis buffer (154 mM NH4Cl, 10 mM KHCO3, 0.1 mM EDTA) and plated in DMEM, 10% FBS, 1% penicillin/streptomycin.

2.6. ECM extraction

SVF-derived ECM was prepared on a protocol based on [14]. Briefly, primary SVF of WT B57Bl/6 mice, aged 7–12 weeks, was plated at 100 000 cells per well (corresponding to a confluence of 80–90% after attachment of cells) on 96-well plates coated with cross-linked gelatin. Regular DMEM with FBS, or DMEM supplemented with FBS and vitamin C (50 μg/μl), was changed every two days. At day 7, ECMs were decellularized by lysing the cells using an alkaline buffer (PBS with 0.5% Triton, 20 mM NH_4OH), followed by at least 8 washes with PBS. To improve ECM purity, nucleotide digestion using benzonase (Merck-Millipore) was performed after the second wash, using 750 U/ml in benzonase buffer, (PBS with 1 mM MgSO4, 1 mM CaCl2), 200ul per well for 30 min at 37 °C.

2.7. FACS

Primary adipose SVF was prepared as described. Cells were stained in FACS buffer (PBS, 3% FBS, 1% penicillin/streptomycin, 1 mM EDTA) for 15 min at 4 °C, washed, strained through 35 μm cell strainers, and sorted on a FACS Diva system (BD). Single stains were done on BD-FACS beads. Fluorescently labeled antibodies (CD45-FITC, CD31-FITC, Ter119-FITC, CD140a-PE, CD34-APC, Sca1-ACP/Cy7) were bought at BioLegend.

2.8. Real-time PCR

mRNA was isolated and transcribed into cDNA using the Multi-MACS cDNA kit (Miltenyi). Expression levels of mRNA were assessed by real-time PCR using SybrGreen (Invitrogen) according to the manufacturer's protocol. Expression was normalized to 36B4.

2.9. Adipocyte differentiation analysis

Differentiated cells were fixed with 4% formaldehyde prior to staining with Hoechst (nuclei), BODIPY (lipid droplets), and Syto60 (cytosol) (Invitrogen). Images were taken per well with an automatic imaging system (Operetta, Perkin Elmer) and analyzed for lipid droplet content using the Operetta software.

2.10. Immunofluorescence

Decellularized ECMs were stained with primary antibodies against fibronectin (Santa Cruz Biotechnology, SC-9086, 1:500), Collagen I, IV and VI (Abcam, ab21286, ab6586 and ab6588, 1:500) at 4 °C overnight, washed with PBS and stained with A488-labeled secondary antibody (Invitrogen, A-21206). Images were taken per well with an automatic imaging system (Operetta, Perkin Elmer).

2.11. Immunoprecipitations

All immunoprecipitations were performed from postconfluent 3T3-L1 cells. Lysis was done in RIPA buffer (50mMTris [pH 7.4], 150mMNaCl, 1% Triton X-100, with 60 mM octyl glucopyranoside), based on [15]. Briefly, cell lysate was incubated overnight at 4 °C on an overhead rotator with 5 μg of antibody (Santa Cruz Biotechnology FLOT2 SC-25507 or rabbit IgG control SC-2027). Next, 60 μl of Protein G-PLUS Agarose (Santa Cruz) (pre-washed twice with RIPA buffer) was incubated with lysate for 2 h at 4 °C on overhead rotator. Agarose beads were washed 5 times (RIPA, 1000 g spin for 2 min between washes), and proteins were eluted in supernatant for western blots in 100 μl of 2× Laemmli buffer (boiled for 10 min before a brief full speed spin to pellet the remaining agarose). For mass spectrometry, agarose beads were transferred to Bio-Spin columns (Bio Rad, #732-6204) for 5 washes with 50 mM ammonium bicarbonate buffer. Proteins were digested overnight at 37 °C with 0.5 μg trypsin in 50 mM ammonium

bicarbonate buffer, and peptides in supernatant were collected and frozen.

2.12. Mass spectrometry

For proteomic experiments, ECMs were grown in 5 ml cell culture dishes. ECM samples were digested in the cell culture dish with 0.5 μg/ul trypsin in ammonium bicarbonate buffer at 37 °C overnight. ECMs were scraped off the plates, sonicated in Eppendorf tubes, digested for another 3 h at 37 °C. Peptides were clarified by centrifugation at 13 000*g* for 10 min.

Trypsin digested samples (ECM or pulldown) were reduced with 5 mM TCEP (tris(2-carboxyethyl)phosphine) and alkylated with 10 mM Iodoacetamide. Peptides were purified with 3–30 μg UltraMicroSpin columns (The Nest Group), dried in a speed-vac, and resolubilized in 0.1% formic acid.

For reversed-phase chromatography a high-performance liquid chromatography (HPLC) column (75-μm inner diameter, New Objective), which was packed in-house with a 15-cm stationary phase (ReproSil-Pur C18-AQ, 1.9 μm, Dr. Maisch), was connected to an EASY-nLC 1000 system (Thermo Scientific). The HPLC was coupled via a nanoelectrospray ion source (Thermo Scientific) to either a Q-exactive plus mass spectrometer (Thermo Scientific; ECM sample data acquisition) or an Orbitrap Fusion tribrid mass spectrometer (Thermo Scientific; FLOT2-IP sample data acquisition. After loading the peptides on the column with 95% buffer A (98% H_2O, 2% acetonitrile, 0.1% formic acid), they were eluted at flow rate of 300 nl/min over a 80 min linear gradient from 5 to 35% buffer B (2% H_2O, 98% acetonitrile, 0.1% formic acid). Mass spectra were acquired in a data-dependent acquisition mode with one cycle consisting of one MS1 scan followed by 10 MS/MS scans.

MSconvert, as part of the Proteowizard (64bit, Version 3.0.6002) package [16] was used to convert raw data into the open mzXL format, which was searched with Comet (2015.01 rev. 2) [17] against the mouse UniProtKB/Swiss-Prot protein databases (release 2014_04). Search parameters for peptide-spectrum matching included cysteine carbamidomethylation (+57.021 Da) as a static amino acid modification as well as methionine, lysine and proline oxidation (+15.995 Da) as variable modification. For probability, scoring of peptides and proteins the Trans-Proteomic Pipeline (Version 4.7) [18] was used including PeptideProphet, ProteinProphet, and protein identifications were filtered to a false-discovery rate of ≤1%. For MS1 based label-free quantification of the identified peptides, MS1 ions signals corresponding to peptide features were extracted with the Progenesis QI for proteomics software (Nonlinear dynamics). After intensity normalization, peptide signal intensities belonging to the same protein were summarized followed by statistical analysis of the data.

2.13. Gene ontology analysis

GO-annotation was performed using the Mus musculus pantherdb database [19].

2.14. Bioethics

All animal studies were approved by the Canton of Zurich Veterinary Office.

2.15. Statistical analysis

Results are given as mean ± standard error. Statistical analyses were performed using a two-tailed Student's *t*-test.

3. RESULTS

3.1. Depot specific differentiation potential is inherent to depot-resident Lin- fibroblasts and Lin- PDGFRα+ populations

Depot specific differences of differentiation potential of preadipocytes from different adipose tissues have been reported in tissues of both human and mouse origin [20–22], with preadipocytes of a Sc origin typically showing higher degrees of differentiation than Vis derived preadipocytes. In contrast, the ex-vivo differentiation capacity of BAT derived preadipocytes has not been compared to that of Sc and Vis derived preadipocytes. Several studies indicate that differences in preadipocyte abundance in Sc and Vis depots are not the cause for altered differentiation capacities. However, this is complicated by the use of surface markers [20,23]. For Lin- PDGFRα+ fibroblasts, which have been shown to be upstream of all mature adipocytes by linage tracing in PDGFRα–Cre:mT/mG mice [5], these comparisons are lacking.

Since the adipocyte niche has also been described to be perivascular and since immune cells have been reported to be important for regulating adipogenesis, we quantified the abundance of endothelial cells (CD45−, CD31+), immune cells (CD45+), and Lin- PDGFRα+ preadipocytes in Sc, Vis, and BAT AT depots (Figure 1A). We found that the Vis AT has a higher content of immune cells than the Sc, and both WAT depots have a higher content than BAT (Figure 1B). CD31+ CD45− endothelial cells are highest in BAT, lower in Sc, and lower still in Vis AT. Inversely, Lin- fibroblasts, known to contain the Lin- PDGFRα+ precursors, are highest in Vis, lower in Sc, and much lower in BAT. In addition, Vis SVF also has a higher percentage of PDGFRα+ within its Lin- population than Sc, and both white depots have a much higher percentage than BAT (Figure 1A).

The marked difference of endothelial and immune cells between Sc and Vis lead us to suspect that the differences in adipogenic potential of the ECMs is modulated by the presence of endothelial or immune cells. Therefore, we isolated the Lin- PDGFRα+ population from WAT and compared its differentiation capacity to complete SVF. As shown in Figure 1C and D, we observed that the differences in differentiation are maintained in these isolated cells, suggesting that the differences in the ex vivo adipogenic potential of SVF from different AT depots reside within the Lin- PDGFRα+ population and does not stem from the contribution of immune cells.

3.2. Addition of vitamin C enhances adipocyte differentiation and orderly deposition of collagens in adipose SVF ex vivo

Preadipocyte differentiation has been shown to be dependent on the production of collagen as well as interaction with ECM [24]. Since vitC is an essential cofactor in the posttranslational modification of collagens, as a first approach to probe for the involvement of ECM in mediating depot specific adipogenesis differences, we differentiated primary SVF of Vis, Sc, and BAT in the presence or absence of vitC (Figure 2A, B). We could show that addition of vitC enhances differentiation in SVF of all three depots and that, as previously reported, Sc SVF differentiates better than Vis, while BAT SVF differentiated much more than both the Sc and Vis derived SVF with vitC. To test whether the antioxidant properties of vitC are responsible for the observed effect, we differentiated 3T3-L1 preadipocytes in the presence of vitamin E (vitE), a strong antioxidant, or vitC. Since only vitC led to an induction of adipogenesis (Figure S1A) we decided to investigate contributions of the ECM on adipogenesis.

In order to test whether the ECM deposited by different SVFs influences differentiation of adipose precursors, we implemented a

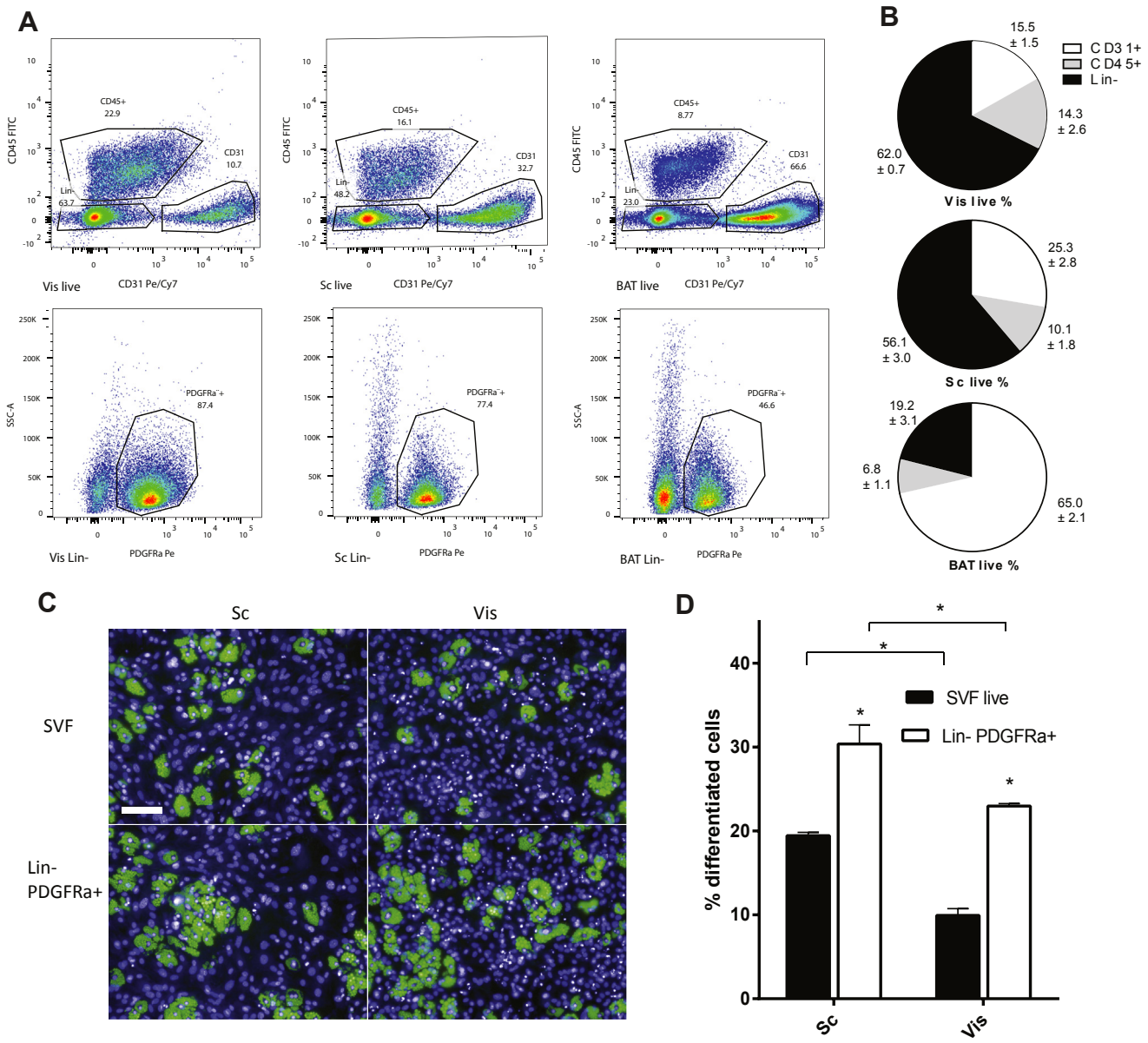

Figure 1: Depot specific differentiation potential is inherent to depot-resident Lin- fibroblasts and Lin- PDGFRα+ populations. (**A**) FACS-analysis of Sc, Vis, and BAT SVF, stained for CD31 (A488), CD45 (PE), PDGFRα (APC) and Sytox Blue. (**B**) Quantification of SVFs for cellular composition (n = 4). (**C**) Differentiation of Sc and Vis Lin- PDGFRα+ cells with vitC; lipid (green) and nuclei (blue) staining. (**D**) Quantification of Lin- PDGFRα+ cell differentiation (n = 4).* $P < 0.05$ by Student's *t*-test. Bar graphs shown are mean ± s.e.m. Scale bar = 100um.

protocol to decellularize primary SVF to obtain SVF-derived ECM. As an initial approach, we performed immunohistochemistry on decellularized primary ECM focusing on fibronectin (FN), as well as two collagens (COL1 and COL4). Fibronectin is one of the most abundant ECM proteins and has been reported to be deposited by fibroblasts very early upon culturing. Collagen I is a collagen belonging to the fibrillar type, being deposited as a broad mesh, and Collagen IV is one of the main components of the basement membrane deposited by endothelial cells. Immunohistochemistry analysis of the ECMs showed that the addition of vitC did not affect the amount or morphology of fibronectin deposition but strongly affected both the amount and the morphology of collagen deposition. VitC increased both the amount of collagen deposition but also the shape of the deposition, with bundles of collagens being more focused and pronounced (Figure 2C). A blatant morphological difference of the vitC ECM is the appearance of a network of elongate bundles of basement membrane collagens (COL1 and COL4) (Figure 2C). We hypothesized these cells to be endothelial cells, and confirmed this by staining with CD31, a well-described endothelial cell marker (Figure S2A). Given the strong visual phenotype of endothelial cell basement membrane collagens on the decellularized ECMs, as well as the fact that in plated SVF, endothelial cells clearly attach and form distinct ECM, we next tested to see how removing endothelial cells affect differentiation of plated SVF. We could show that removing endothelial cells from SVF by FACS-sorting, CD31- cells enhanced differentiation in both tissues (Figure 2D,E) to an extent that was similar to plated Lin- PDGFRα+

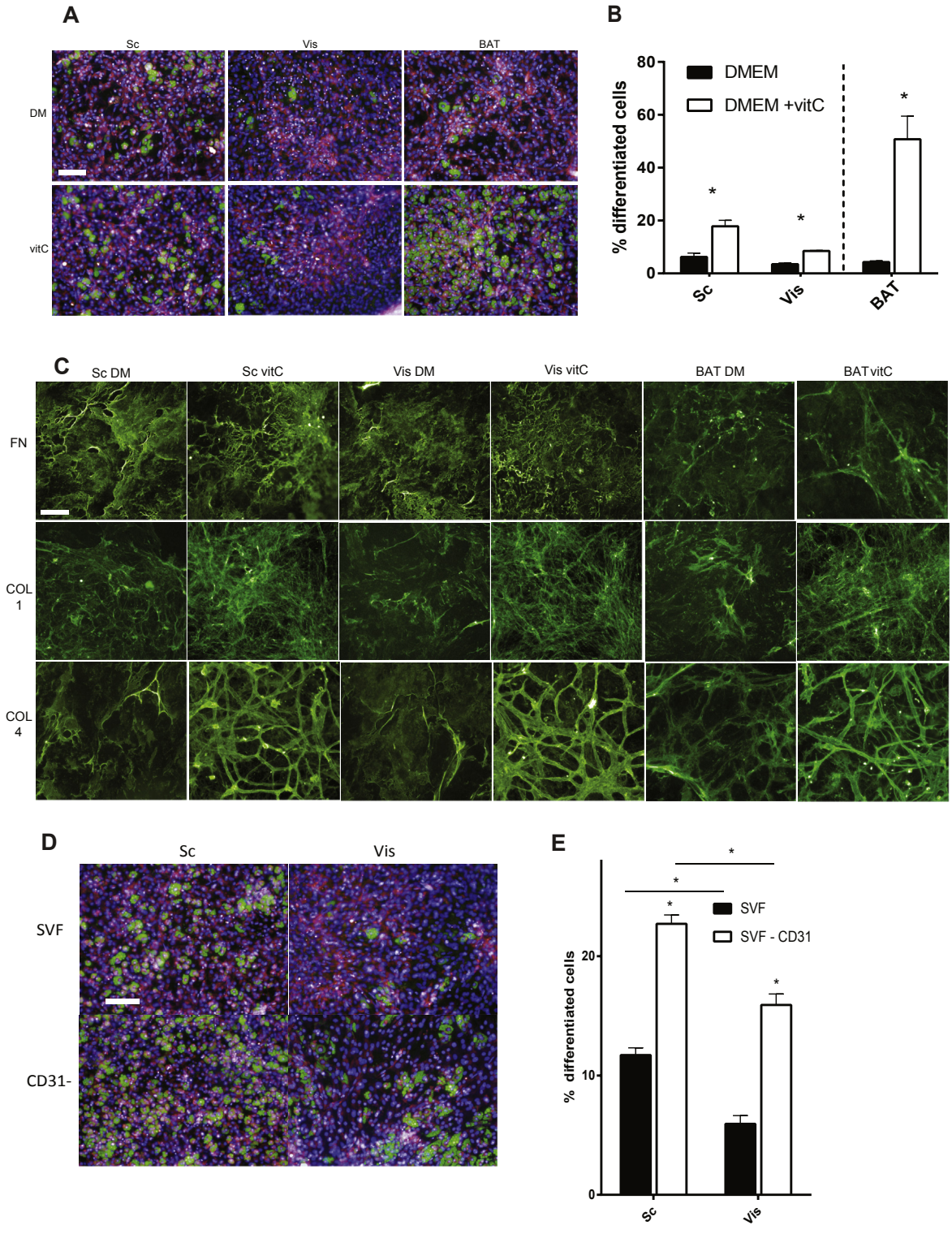

Figure 2: Addition of vitamin C enhances adipocyte differentiation and orderly deposition of collagens in adipose SVF ex vivo. SVF of Sc, Vis, and BAT differentiated in the presence and absence of vitC. (**A**) Representative images: lipid (green), nuclei (blue), and cytosol (pink) staining. (**B**) Quantification. (**C**) Images of decellularized ECM of Sc, Vis, and BAT SVF, stained for Collagen I (COL1), Fibronectin (FN), and Collagen VI (COL4), with Alexa 488 (green). (**D**) SVF of Sc and Vis differentiated in the presence of vitC with and without depletion of CD31+ cells. Lipid (green), nuclei (blue), and cytosol (pink) staining. (**E**) Quantification of SVF differentiated with and without CD31+ cell depletion (n = 4). * $P < 0.05$, ** $P < 0.01$ by Student's *t*-test. Bar graphs shown are mean ± s.e.m. Scale bar = 100um.

SVF (Figure 1C,D). Nevertheless, the depot specific differences were retained (Figure 2D,E), corroborating our finding that Lin+ cells are not responsible for the observed depot specific differences ex vivo.

3.3. SVF-derived ECM modulates differentiation capacity of adipocyte precursor cells

In order to unequivocally test whether the ECM deposited by different SVFs influences differentiation of adipose precursors, we implemented a protocol to reseed primary, FACS-sorted adipose Lin-PDGFRα+ precursors into decellularized, primary SVF-derived ECM (Figure 3A) and induce differentiation. Since Vis AT has the highest amount of these cells and since Vis SVF shows the lowest amount of differentiation (Figure 2B), we analyzed the capacity of Vis Lin-PDGFRα+ adipocyte precursors to differentiate in ECM environments from all three depots. We found that the origin of the ECM largely recapitulated the differences in differentiation observed in different tissue SVF, as Vis precursors differentiated better in Sc and BAT than Vis ECM (Figure 3B). To quantify the effects, we extracted RNA from reseeded cells after 2 days of differentiation and measured levels of PPARγ and FABP4, two proteins, which are induced early in adipocyte differentiation. Reseeding adipocyte precursors into their respective ECMs shows that ECMs grown with added vitC enhance differentiation (Figure 3C,D). Measuring FABP4 and PPARγ levels from Vis precursors in all three ECMs, grown with added vitC, confirmed our observation that BAT ECM is more adipogenic than ECMs from both WAT depots (Figure 3E). Taken together, our data indicate that the ECM environment provided by the SVF influences the differentiation behavior of preadipocytes ex vivo and recapitulates the capacity of SVF from different AT depots to differentiate, ex vivo.

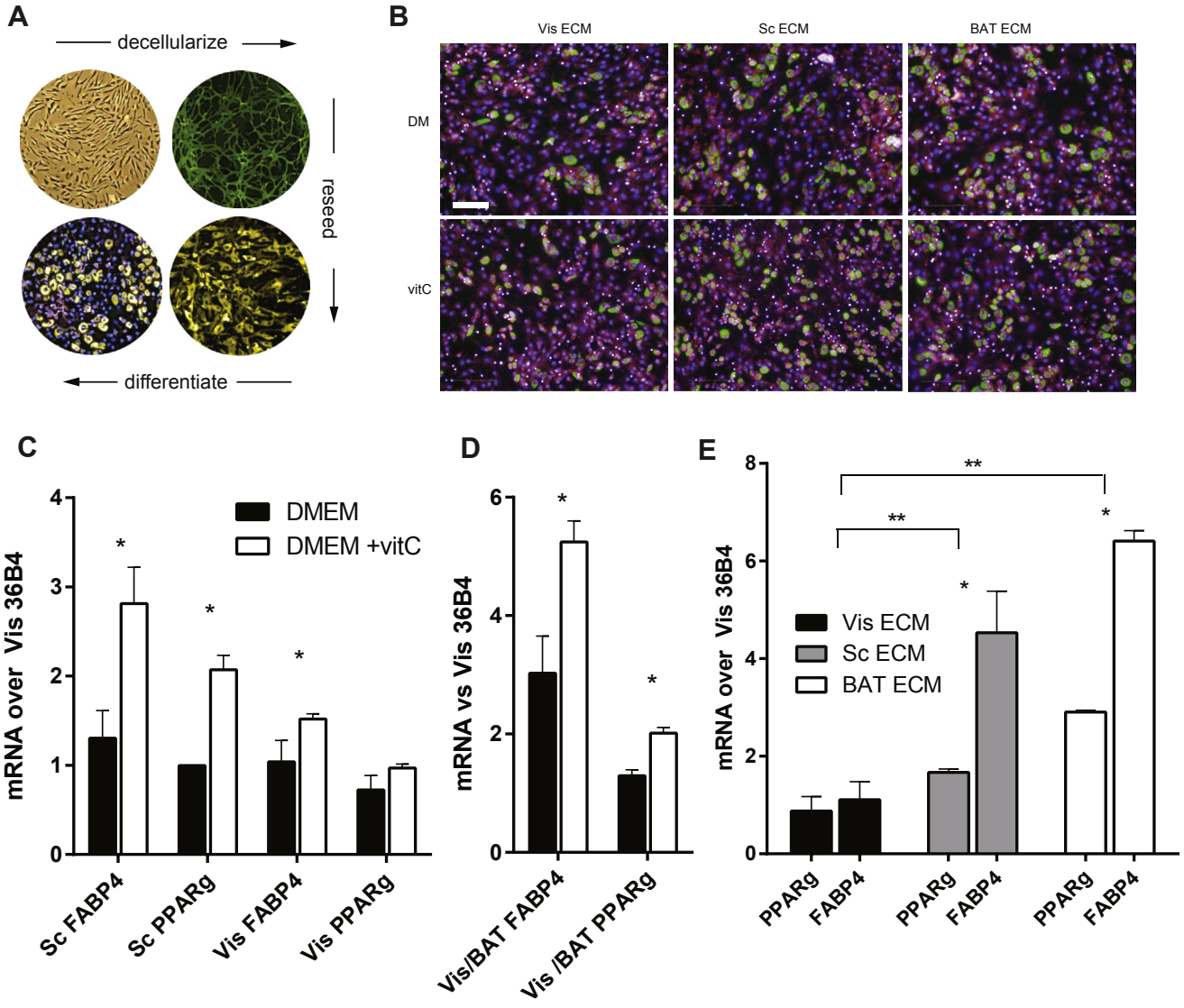

Figure 3: SVF-derived ECM modulates differentiation capacity of adipose stem cells. (**A**) Scheme of SVF-decellularization and reseeding with FACS-sorted adipocyte precursors. (**B**) Lin- PDGFRα+ Vis adipocyte precursor cells differentiated in ECMs ± vitC, representative images: lipid (green), nuclei (blue), and cytosol (pink) staining. (**C**–**E**) qPCR for FABP4 and PPARγ of RNA extracted from differentiating precursors. (**C**) Lin- PDGFRα+ seeded into ECM ± vitC (n = 3). (**D**) Vis Lin- PDGFRα+ cells seeded into BAT ECMs ± vitC. (n = 3). (**E**) Vis Lin- PDGFRα+ cells seeded into BAT ECMs +vitC of Sc, Vis and BAT. (n = 3) * $P < 0.05$ by Student's *t*-test, Bar graphs shown are mean ± s.e.m. Scale bar = 100um.

3.4. Proteomic analysis of SVF-derived ECM

In order to elucidate the different effect of SVF-ECM on preadipocyte differentiation, we performed label-free shotgun proteomics of Sc, Vis, and BAT grown with and without added vitC. We detected peptides mapping to more than 1600 different proteins over all three tissues. The two most abundant proteins in all samples were fibronectin (FN) and collagen 1 (COL1), which were generated in the presence and absence of vitC, respectively (Figure 4A, Supplementary Table 1). Highly abundant proteins not regulated by vitC were ECM proteins such as fibrillin and vimentin and components of the cytoskeleton like actin or myosin, which still adhere to decellularized membrane. While the different depots showed similar compositions, addition of vitC caused a marked increase of the amount of detected collagens (but no shift in types), concomitant with collagen-associated extracellular proteins, most prominently periostin, biglycan, and decorin. Gene-Ontology analysis of all detected proteins mapped a number of detected proteins to compartments other than the ECM (Figure 4B). This is partly due to contamination of cytosolic proteins that were non-specifically attached to the decellularized ECMs, most prominently histones, ribosomal proteins, and heat-shock proteins, which are known contaminants in protein interaction studies [25]. It also partly reflects the fact that the functional interactions between the ECM and cells seem to partially stay attached during decellularization, accounting for the presence of cytolinker and cytoskeletal proteins. When analyzing the differences in ECM composition between the different depots, our datasets revealed a large overlap in the proteome between the different depots (Figure 4C), with that derived from BAT having a more unique protein signature than the two WAT depots. Collectively, these data show that addition of vitC causes a strong increase in collagen deposition on SVF-derived ECMs and a conserved core of proteins abundant in all adipose SVF-derived ECMs.

3.5. Flotillin 2 is enriched in pro-adipogenic ECM and mediates vitC dependent effects on differentiation

One protein that was consistently upregulated in +vitC ECMs, to a level similar to collagens, was Flotillin 2 (FLOT2). Therefore, we analyzed whether FLOT2 was also differentially regulated between the three depots. Indeed, we found significantly higher levels of FLOT2 in Sc and BAT ECM compared to Vis (Figure 5A). In contrast, FLOT2 expression in vivo, by Western Blot analysis of whole tissue extract, was unchanged (Figure S3A), which is probably due to the fact that FLOT2 is ubiquitously expressed. FLOT2 is a transmembrane protein localized to lipid rafts in the plasma membrane. This cellular localization, combined with the proteome-data, prompted us to speculate that FLOT2 plays a role in organizing the signaling machinery necessary to interpret specific ECM to cell signaling cues. To further understand the role of FLOT2, we performed co-Immunoprecipitation (co-IP) assays against FLOT2 in 3T3-L1 cells and analyzed the precipitated proteins by mass spectroscopy, followed by running an algorithm designed to remove false interactions commonly detected in co-IP assays [26] (Figure S3B,C). GO-analysis of detected proteins revealed them to map to signaling pathways such as integrin signaling, axon guidance pathways, Ras, and cytoskeletal Rho signaling, which is consistent with our hypothesis (Figure 5B). Therefore, in order to test the functional involvement of FLOT2 in the differentiation process, we used siRNA mediated knock down of FLOT2 in 3T3-L1 preadipocytes (Figure S3D) and differentiated them in the presence and absence of vitC. Interestingly, ablation of FLOT2 completely abolished the effect of vitC on adipocyte differentiation (Figure 5C,D) suggesting that this protein might indeed be one responsible factor mediating the effects of ECM on adipocyte differentiation potential. In summary, we found that FLOT2 is differently regulated in decellularized ECMs of different depots, with more pro-adipogenic ECMs showing much higher levels of FLOT2, and necessary for vitC enhanced differentiation in vivo, suggesting that it plays an important role in mediating the signaling of different ECM properties.

4. DISCUSSION

In this study, we show that the ECM of primary AT SVF directly influences differentiation of adipogenic precursors, which provides an explanation for existing findings that cells of distinct adipose depots show varying capacities for differentiating into mature adipocytes.

Interestingly, Lin- PDGFRα+ cells, which have been shown to contain adipocyte precursors [5,6], are significantly more abundant in Vis than Sc adipose tissue, even though Sc Lin- PDGFRα+ cells have repeatedly been demonstrated to have a higher rate of differentiation than Vis derived cells [20,23]. Two recent studies focusing on adipose tissue expansion during the very early time-points of obesity development (three days and two weeks of high fat diet (HFD) feeding) [27,28], on the other hand, demonstrate that cell division and BrdU incorporation almost exclusively occur in Vis, but not Sc adipose tissue. Based on these data, it has been speculated that HFD feeding triggers local and systemic changes that cause an activation of the stem cell pool in adipose tissue and triggers proliferation and differentiation of preadipocytes. This is supported by a recent study, which demonstrated that blocking inflammation, specifically in the adipose tissue, leads to reduced adipogenesis upon high fat diet feeding and a more unfavorable systemic metabolic outcome, suggesting that inflammatory processes are involved in such a regulation [29]. Related to this, an adipogenic niche consisting of PDGFRα+ fibroblasts expressing the osteopontin receptor CD44, as well as M2 polarized macrophages secreting osteopontin, was recently identified, and it was demonstrated that proliferation of these cells is enhanced in Vis over Sc adipose tissue upon triggering adipocyte hyperplasia [30]. Another study, comparing hyperplasia between Sc and Vis AT demonstrated more increased hyperplasia and turnover in the Vis than the Sc AT [31], in addition to showing that Sc AT is more easily exhaustible than Vis AT. These data taken together with our findings suggest that not the precursors themselves present in AT, but rather the microenvironment, which is shaped by the ECM can confer the signal required to induce adipogenesis.

Furthermore, based on this compilation of data, it is tempting to speculate that the Lin- PDGFRα+ cell population contains a niche cell population which signals to maintain stemness and proliferative potential of precursor cells and blocks differentiation. Such a population would have to be more abundant in Vis AT than in Sc AT or BAT and would respond to dietary cues such as lipids derived from the diet. A better characterization of the Lin- PDGFRα+ subpopulations will be needed to identify such cells.

Furthermore, our data of EMCs grown with and without vitamin C suggest that collagens play an essential role in conferring these properties, a finding that is in line with recent findings in vivo [32]. One caveat when interpreting our findings is the fact that cells seeded into the ECM themselves will modulate the matrix and thus contribute to the observed phenotype.

Most cells require stable cell-matrix adhesion contacts for survival and proper function. The canonical pathways for ECM to cell signaling at the plasma membrane are focal adhesion kinase (FAK) and integrin-linked kinase (ILK). In addition, the transcription factors YAP and TAZ have

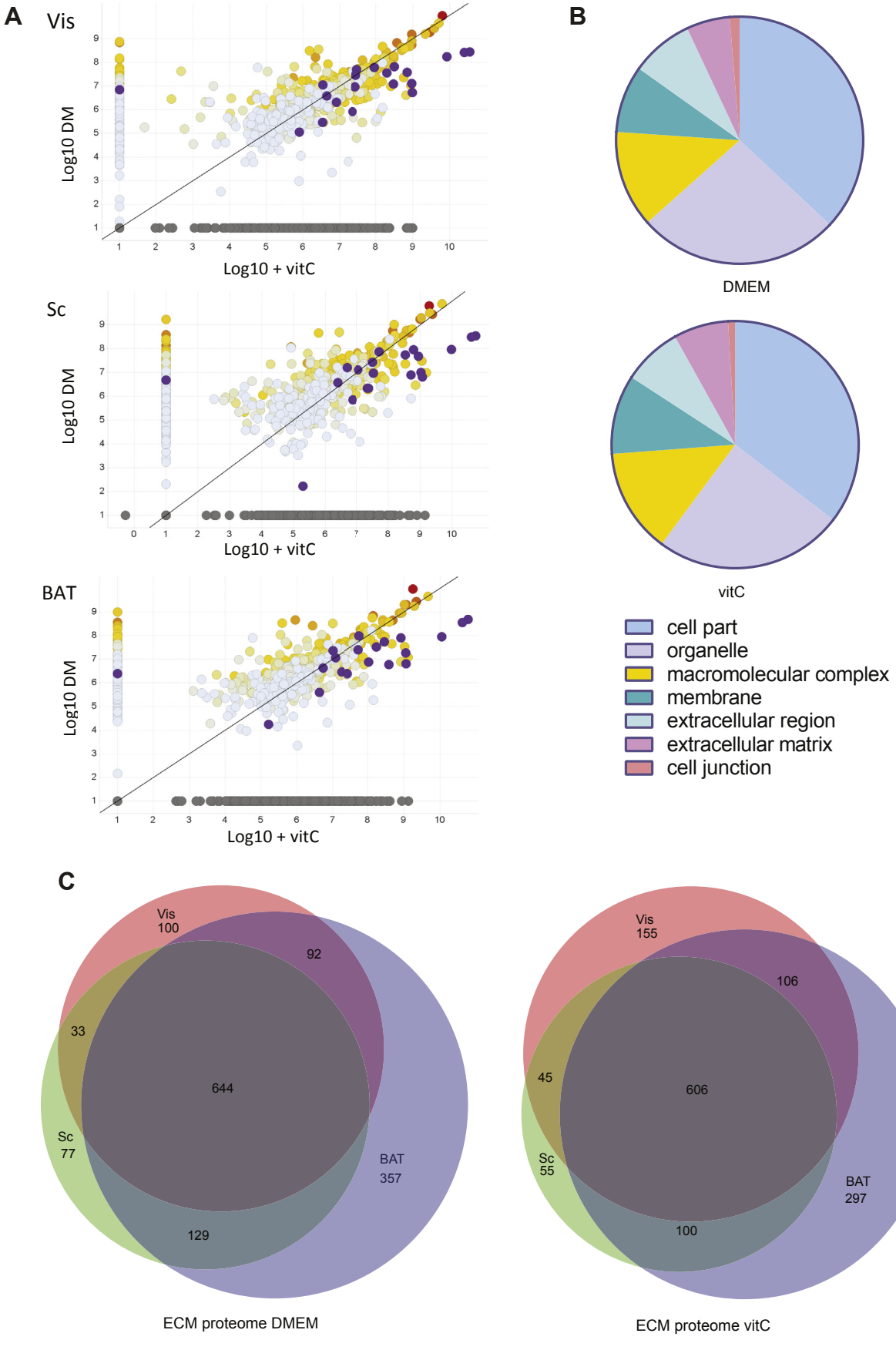

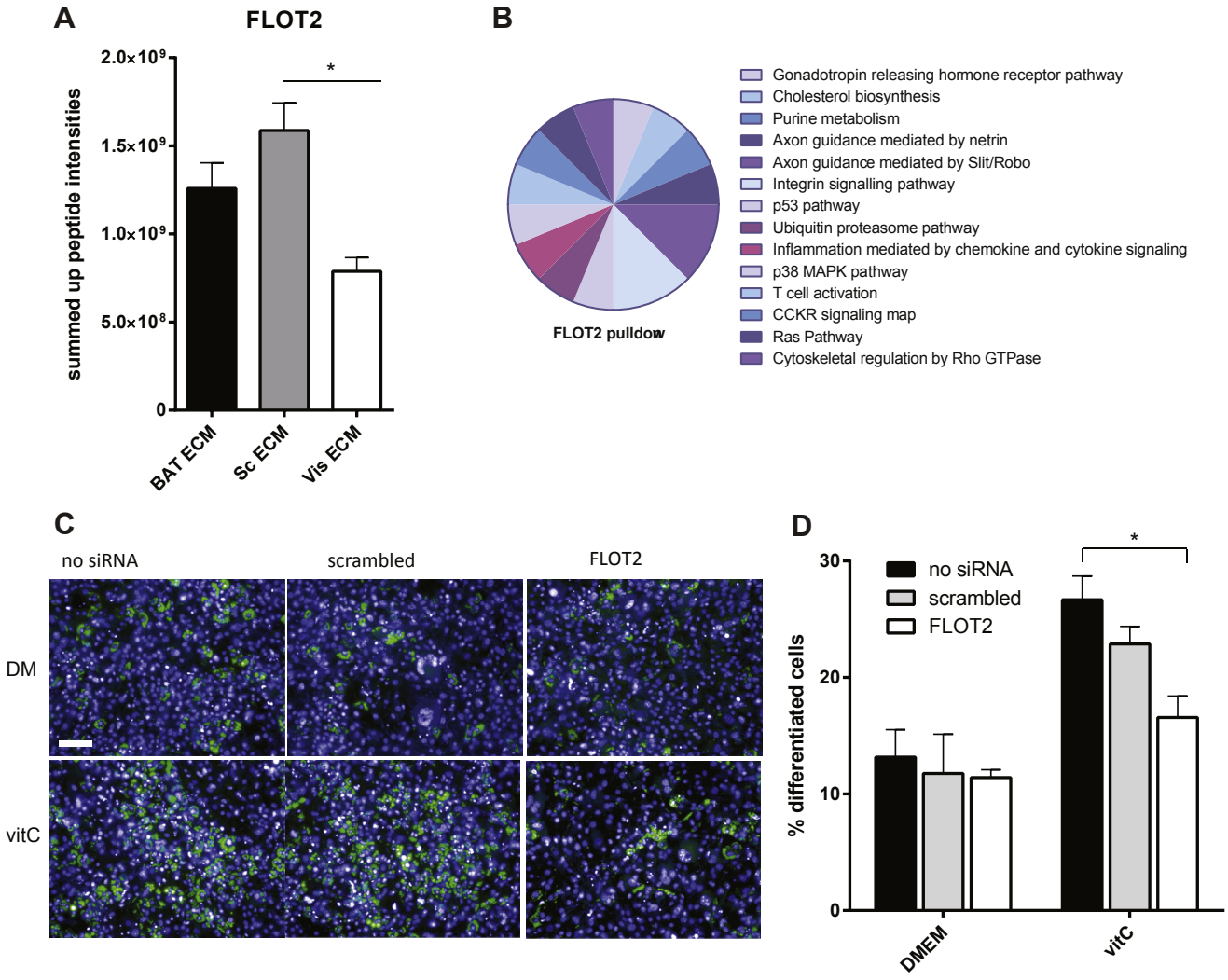

Figure 5: Flotillin 2 is enriched in pro-adipogenic ECM and mediates vitC dependent effects on differentiation. (**A**) Summed up peptide intensities of FLOT2 in decellularized ECMs of Sc, Vis, and BAT grown in DMEM +vitC. (**B**) Panther-classifications of the signaling pathways of detected FLOT2 interacting proteins (n = 4). (**C**) 3T3 cells differentiated in the presence and absence of vitC with siRNA against FLOT2 (n = 3). (**D**) Representative images: lipid (green) and nucleus (blue) staining of differentiated 3T3-cells. Bar graphs shown are mean ± s.e.m. * $P < 0.05$ by Student's *t*-test. Bar graphs shown are mean ± s.e.m. Scale bar = 100um.

recently been shown to play an important role in regulation the signaling machinery for sensing and reacting to different matrix stiffness cues [33]. However, knockdowns of these factors, while affecting differentiation of 3T3-L1 cells compared to unspecific siRNAs, do not modulate the collagen dependent vitC response (Figure S1A), suggesting that the collagen dependent effect of ECMs we observe in preadipocytes from different depots is probably not mediated by these proteins.

In addition to the matrix functionalities such as receptor binding motifs, growth factor sequestering, or protease dependent release of signaling peptides, matrix stiffness of the ECM is an important property [34,35]. Recent findings suggest that an important factor contributing to stiffness sensing, however, may just lead to changes in the availability of binding sites for mechanosensing complexes on matrices with larger pore sizes [36]. While we did not investigate mechanical properties, we found the plasma transmembrane and lipid raft associated protein FLOT2 to be regulated in accordance with the adipogenicity of adipose depot-derived ECMs. FLOT2 is associated to the plasma membrane by two n-terminal transmembrane hairpin loops as well as n-terminal myristoylation and palmitoylation, while the c-terminus is cytosolic. FLOT2 and its homolog FLOT1 were first described in regenerating ganglion cells and independently identified as proteins in detergent resistant membrane fractions that float in density gradients [37,38]. Because of their prominent role in lipid raft formation, Flotillins have been studied in the context of cell proliferation, migration, and cell—cell interaction, and they have been shown to interact or associate with both cell surface signaling molecules GPCRs [39], receptor tyrosine

Figure 4: Proteomic analysis of SVF-derived ECM does not reveal a strong depot specific signature. (**A**) Scatter plots of detected proteins in SVF-derived ECM of Sc, Vis, and BAT, grown in DMEM and DMEM +vitC, showing fibronectin (red), collagens (purple), and other proteins (hues of yellow, grey and blue). Log10 scale, non-detected samples (0) are set to 1. (**B**) Panther classification — Annotations of all proteins detected in the three tissues, grown with and without added vitC. (**C**) Venn-Diagrams of SVF-ECM from Sc, Vis and BAT grown in DMEM and DMEM + vitC.

kinases, and intracellular actin binding proteins such as myosin [40] or γ-catenin [41].

Interestingly, while we found a roughly 2-fold increase of FLOT2 in pro-adipogenic ECMs, FLOT1 abundance was not changed, suggesting a differential regulation of certain membrane microdomains in relation to matrix composition and assembly. We hypothesize that FLOT2 might organize a matrix signaling hub integrating a variety of ECM signals. Our co-IP data support this interpretation even in light of the fact that we performed co-IP with an antibody against an endogenous transmembrane protein, which is a detergent-resistant microdomain-protein, and thus might have a limited coverage. A recently published paper outlined a human interactome by performing co-IPs for a wide range of cellular targets using GFP-tagged overexpressed proteins and computationally matching mutual hits. This paper reports that FLOT2 interacts with a variety of small GTPases and G-protein subunits as well as with actin binding proteins implicated in mechanosensing, cytoskeletal dynamics, and cell motility, lending further support to our hypothesis that FLOT2-dependent signaling contributes to sensing and interpreting ECM properties [42].

In summary, we demonstrate that the depot specific differences of the potential of adipocyte precursors to form mature adipocytes is mainly dependent on the ECM and that integration of the necessary ECM to cell signaling cues might in part be mediated through transmembrane protein Flot2.

AUTHOR CONTRIBUTIONS

G.G. developed the hypothesis, performed experimental work, analyzed the data, and wrote the manuscript. B.W. supervised the proteomic experiments. S.M. and H.M. performed mass spectrometric data acquisition and analysis. C.M. performed experimental work and analyzed data, and C.W. initiated and supervised the project, analyzed the data and wrote the manuscript.

ACKNOWLEDGMENTS

We wish to thank M. Geiger and E. Kiehlmann and Alexandra Fahrner for technical help. We also wish to thank for Nigel Beaton helpful discussions. This work was supported by the Schering Foundation (G.G.) and the SNF (CW).

CONFLICT OF INTEREST

The authors declare no competing financial interests.

APPENDIX A. SUPPLEMENTARY DATA

Supplementary data related to this article can be found at http://dx.doi.org/10.1016/j.molmet.2016.07.008.

REFERENCES

[1] NCD Risk Factor Collaboration, 2016. Trends in adult body-mass index in 200 countries from 1975 to 2014: a pooled analysis of 1698 population-based measurement studies with 19·2 million participants. The Lancet 387(10026):1377–1396. http://dx.doi.org/10.1016/S0140-6736(16)30054-X.

[2] Rosen, E.D., Spiegelman, B.M., 2014. What we talk about when we talk about fat. Cell 156(1–2):20–44. http://dx.doi.org/10.1016/j.cell.2013.12.012.

[3] Tang, W., Zeve, D., Suh, J.M., Bosnakovski, D., Kyba, M., Hammer, R.E., et al., 2008. White fat progenitor cells reside in the adipose vasculature. Science (New York, N.Y.) 322(October):583–586. http://dx.doi.org/10.1126/science.1156232.

[4] Rodeheffer, M.S., Birsoy, K., Friedman, J.M., 2008. Identification of white adipocyte progenitor cells in vivo. Cell 135(2):240–249. http://dx.doi.org/10.1016/j.cell.2008.09.036.

[5] Berry, R., Rodeheffer, M.S., 2013. Characterization of the adipocyte cellular lineage in vivo. Nature Cell Biology 15(3):302–308. http://dx.doi.org/10.1038/ncb2696.

[6] Lee, Y.-H., Petkova, A.P., Mottillo, E.P., Granneman, J.G., 2012. In vivo identification of bipotential adipocyte progenitors recruited by β3-adrenoceptor activation and high-fat feeding. Cell Metabolism 15(4):480–491. http://dx.doi.org/10.1016/j.cmet.2012.03.009.

[7] Tontonoz, P., Hu, E., Spiegelman, B.M., 1994. Stimulation of adipogenesis in fibroblasts by PPAR gamma 2, a lipid-activated transcription factor. Cell 79(7):1147–1156.

[8] Kubo, Y., Kaidzu, S., Nakajima, I., Takenouchi, K., Nakamura, F., 2000. Organization of extracellular matrix components during differentiation of adipocytes in long-term culture. In Vitro Cellular & Developmental Biology. Animal 36(January):38–44. http://dx.doi.org/10.1290/1071-2690(2000)036<0038:OOEMCD>2.3.CO;2.

[9] Chun, T.-H., Hotary, K.B., Sabeh, F., Saltiel, A.R., Allen, E.D., Weiss, S.J., 2006. A pericellular collagenase directs the 3-dimensional development of white adipose tissue. Cell 125(3):577–591. http://dx.doi.org/10.1016/j.cell.2006.02.050.

[10] Watt, F.M., Huck, W.T.S., 2013. Role of the extracellular matrix in regulating stem cell fate. Nature Reviews. Molecular Cell Biology 14(8):467–473. http://dx.doi.org/10.1038/nrm3620.

[11] Sun, K., Tordjman, J., Clément, K., Scherer, P.E., 2013. Fibrosis and adipose tissue dysfunction. Cell Metabolism 18(4):470–477. http://dx.doi.org/10.1016/j.cmet.2013.06.016.

[12] Tchkonia, T., Thomou, T., Zhu, Y., Karagiannides, I., Pothoulakis, C., Jensen, M.D., et al., 2013. Mechanisms and metabolic implications of regional differences among fat depots. Cell Metabolism 17(5):644–656. http://dx.doi.org/10.1016/j.cmet.2013.03.008.

[13] Meissburger, B., Ukropec, J., Roeder, E., Beaton, N., Geiger, M., Teupser, D., et al., 2011. Adipogenesis and insulin sensitivity in obesity are regulated by retinoid-related orphan receptor gamma. EMBO Molecular Medicine 3(11):637–651. http://dx.doi.org/10.1002/emmm.201100172.

[14] Beacham, D.A., Amatangelo, M.D., Cukierman, E., 2007. Preparation of extracellular matrices produced by cultured and primary fibroblasts. Current Protocols in Cell Biology/Editorial Board. http://dx.doi.org/10.1002/0471143030.cb1009s33. Juan S. Bonifacino… [et al.] Chapter 10: Unit 10.9.

[15] Frick, M., Bright, N.A., Riento, K., Bray, A., Merrified, C., Nichols, B.J., 2007. Coassembly of Flotillins induces formation of membrane microdomains, membrane curvature, and vesicle budding. Current Biology 17(13):1151–1156. http://dx.doi.org/10.1016/j.cub.2007.05.078.

[16] Chambers, M.C., Maclean, B., Burke, R., Amodei, D., Ruderman, D.L., Neumann, S., et al., 2012. A cross-platform toolkit for mass spectrometry and proteomics. Nature Biotechnology 30(10):918–920. http://dx.doi.org/10.1038/nbt.2377.

[17] Eng, J.K., Jahan, T.A., Hoopmann, M.R., 2013. Comet: an open-source MS/MS sequence database search tool. Proteomics 13(1):22–24. http://dx.doi.org/10.1002/pmic.201200439.

[18] Deutsch, E.W., Mendoza, L., Shteynberg, D., Farrah, T., Lam, H., Tasman, N., et al., 2010. A guided tour of the trans-proteomic pipeline. Proteomics 10(6):1150–1159. http://dx.doi.org/10.1002/pmic.200900375.

[19] Mi, H., Muruganujan, A., Casagrande, J.T., Thomas, P.D., 2013. Large-scale gene function analysis with the PANTHER classification system. Nature Protocols 8(8):1551–1566. http://dx.doi.org/10.1038/nprot.2013.092.

[20] Macotela, Y., Emanuelli, B., Mori, M.A., Gesta, S., Schulz, T.J., Tseng, Y.H., et al., 2012. Intrinsic differences in adipocyte precursor cells from different white fat depots. Diabetes 61(7):1691–1699. http://dx.doi.org/10.2337/db11-1753.

[21] Tchkonia, T., Giorgadze, N., Pirtskhalava, T., Thomou, T., DePonte, M., Koo, A., et al., 2006. Fat depot-specific characteristics are retained in strains derived from single human preadipocytes. Diabetes 55(9):2571–2578. http://dx.doi.org/10.2337/db06-0540.

[22] Meissburger, B., Perdikari, A., Moest, H., Müller, S., Geiger, M., Wolfrum, C., 2016. Regulation of adipogenesis by paracrine factors from adipose stromal-vascular fraction - a link to fat depot-specific differences. Biochimica et Biophysica Acta (BBA) – Molecular and Cell Biology of Lipids. http://dx.doi.org/10.1016/j.bbalip.2016.06.010.

[23] Joe, A.W.B., Yi, L., Even, Y., Vogl, A.W., Rossi, F.M.V., 2009. Depot-specific differences in adipogenic progenitor abundance and proliferative response to high-fat diet. Stem Cells (Dayton, Ohio) 27(10):2563–2570. http://dx.doi.org/10.1002/stem.190.

[24] Nakajima, I., Muroya, S., Tanabe, R.I., Chikuni, K., 2002. Positive effect of collagen V and VI on triglyceride accumulation during differentiation in cultures of bovine intramuscular adipocytes. Differentiation 70(2–3):84–91. http://dx.doi.org/10.1046/j.1432-0436.2002.700203.x.

[25] Trinkle-Mulcahy, L., Boulon, S., Lam, Y.W., Urcia, R., Boisvert, F.M., Vandermoere, F., et al., 2008. Identifying specific protein interaction partners using quantitative mass spectrometry and bead proteomes. Journal of Cell Biology 183(2):223–239. http://dx.doi.org/10.1083/jcb.200805092.

[26] Choi, H., Larsen, B., Lin, Z., Breitkreutz, A., Fermin, D., Qin, Z.S., et al., 2011. NIH Public Access 8(1):70–73. http://dx.doi.org/10.1038/nmeth.1541.SAINT.

[27] Jeffery, E., Church, C.D., Holtrup, B., Colman, L., Rodeheffer, M.S., 2015. Rapid depot-specific activation of adipocyte precursor cells at the onset of obesity. Nature Cell Biology 17(4):376–385. http://dx.doi.org/10.1038/ncb3122.

[28] Wang, Q.A., Tao, C., Gupta, R.K., Scherer, P.E., 2013. Tracking adipogenesis during white adipose tissue development, expansion and regeneration. Nature Medicine 19(10):1338–1344. http://dx.doi.org/10.1038/nm.3324.

[29] Wernstedt Asterholm, I., Tao, C., Morley, T.S., Wang, Q.A., Delgado-Lopez, F., Wang, Z.V., et al., 2014. Adipocyte inflammation is essential for healthy adipose tissue expansion and remodeling. Cell Metabolism 20(1):103–118. http://dx.doi.org/10.1016/j.cmet.2014.05.005.

[30] Lee, Y.-H., Petkova, A.P., Granneman, J.G., 2013. Identification of an adipogenic niche for adipose tissue remodeling and restoration. Cell Metabolism 18(3):355–367. http://dx.doi.org/10.1016/j.cmet.2013.08.003.

[31] Kim, S.M., Lun, M., Wang, M., Senyo, S.E., Guillermier, C., Patwari, P., 2014. Article loss of white adipose hyperplastic potential is associated with enhanced susceptibility to insulin resistance. Cell Metabolism 20(6):1049–1058. http://dx.doi.org/10.1016/j.cmet.2014.10.010.

[32] Khan, T., Muise, E.S., Iyengar, P., Wang, Z.V., Chandalia, M., Abate, N., et al., 2009. Metabolic dysregulation and adipose tissue fibrosis: role of collagen VI. Molecular and Cellular Biology 29(6):1575–1591. http://dx.doi.org/10.1128/MCB.01300-08.

[33] Dupont, S., Morsut, L., Aragona, M., Enzo, E., Giulitti, S., Cordenonsi, M., et al., 2011. Role of YAP/TAZ in mechanotransduction. Nature 474(7350):179–183. http://dx.doi.org/10.1038/nature10137.

[34] Vogel, V., Sheetz, M., 2006. Local force and geometry sensing regulate cell functions. Nature Reviews. Molecular Cell Biology 7(4):265–275. http://dx.doi.org/10.1038/nrm1890.

[35] Elosegui-Artola, A., Bazellières, E., Allen, M.D., Andreu, I., Oria, R., Sunyer, R., et al., 2014. Rigidity sensing and adaptation through regulation of integrin types. Nature Materials 13(6):631–637. http://dx.doi.org/10.1038/nmat3960.

[36] Trappmann, B., Gautrot, J.E., Connelly, J.T., Strange, D.G.T., Li, Y., Oyen, M.L., et al., 2012. Extracellular-matrix tethering regulates stem-cell fate. Nature Materials 11(7):642–649. http://dx.doi.org/10.1038/nmat3339.

[37] Schulte, T., Paschke, K.A., Laessing, U., Lottspeich, F., Stuermer, C.A., 1997. Reggie-1 and reggie-2, two cell surface proteins expressed by retinal ganglion cells during axon regeneration. Development (Cambridge, England) 124(2):577–587.

[38] Bickel, P.E., Scherer, P.E., Schnitzer, J.E., Oh, P., Lisanti, M.P., Lodish, H.F., 1997. Flotillin and epidermal surface antigen define a new family of caveolae-associated integral membrane proteins. The Journal of Biological Chemistry 272(21):13793–13802. http://dx.doi.org/10.1074/jbc.272.21.13793.

[39] Hazarika, P., Mccarty, M.F., Prieto, V.G., Bar-eli, M., Duvic, M., 2004. Up-regulation of Flotillin-2 is associated with melanoma progression and modulates expression of the thrombin receptor protease activated receptor 1. p. 7361–9. http://dx.doi.org/10.1158/0008-5472.CAN-04-0823.

[40] Otto, G.P., Nichols, B.J., 2011. The roles of flotillin microdomains - endocytosis and beyond. Journal of Cell Science 124(23):3933–3940. http://dx.doi.org/10.1242/jcs.092015.

[41] Kurrle, N., Völlner, F., Eming, R., Hertl, M., Banning, A., Tikkanen, R., 2013. Flotillins directly interact with γ-catenin and regulate epithelial cell-cell adhesion. PLoS One 8(12). http://dx.doi.org/10.1371/journal.pone.0084393.

[42] Hein, M.Y., Hubner, N.C., Poser, I., Cox, J., Nagaraj, N., Toyoda, Y., et al., 2015. A human interactome in three quantitative dimensions organized by stoichiometries and abundances. Cell 163(3):712–723. http://dx.doi.org/10.1016/j.cell.2015.09.053.

